american physiological society®

AMERICAN JOURNAL OF PHYSIOLOGY
RENAL PHYSIOLOGY®

Am J Physiol Renal Physiol 324: F571–F580, 2023.
First published April 27, 2023; doi:10.1152/ajprenal.00294.2022

RESEARCH ARTICLE

Control of Renal Function in Health and Disease Conference 2022

Renal mitochondrial dysfunction in ovine experimental sepsis-associated acute kidney injury

Tomas Luther,[1] Sara Bülow-Anderberg,[1] Patrik Persson,[2] Stephanie Franzén,[1] Paul Skorup,[3] Annika Wernerson,[4] Kjell Hultenby,[5] Fredrik Palm,[2] Tomas A. Schiffer,[6] and Robert Frithiof[1]

[1]*Department of Surgical Sciences, Anesthesiology and Intensive Care, Uppsala University, Uppsala, Sweden;* [2]*Section of Integrative Physiology, Department of Medical Cell Biology, Uppsala University, Uppsala, Sweden;* [3]*Section of Infectious Diseases, Department of Medical Sciences, Uppsala University, Uppsala, Sweden;* [4]*Division of Renal Medicine, Department of Clinical Science, Intervention and Technology, Karolinska Institutet, Stockholm, Sweden;* [5]*Division of Biomolecular and Cellular Medicine, Department of Laboratory Medicine, Karolinska Institutet, Stockholm, Sweden; and* [6]*Department of Physiology and Pharmacology, Karolinska Institutet, Stockholm, Sweden*

Abstract

Sheep develop sepsis-associated acute kidney injury (SA-AKI) during experimental sepsis despite normal to increased renal oxygen delivery. A disturbed relation between oxygen consumption ($\dot{V}O_2$) and renal Na^+ transport has been demonstrated in sheep and in clinical studies of AKI, which could be explained by mitochondrial dysfunction. We investigated the function of isolated renal mitochondria compared with renal oxygen handling in an ovine hyperdynamic model of SA-AKI. Anesthetized sheep were randomized to either an infusion of live *Escherichia coli* with resuscitative measures (sepsis group; n = 13 animals) or served as controls (n = 8 animals) for 28 h. Renal $\dot{V}O_2$ and Na^+ transport were repeatedly measured. Live cortical mitochondria were isolated at baseline and at the end of the experiment and assessed in vitro with high-resolution respirometry. Sepsis markedly reduced creatinine clearance, and the relation between Na^+ transport and renal $\dot{V}O_2$ was decreased in septic sheep compared with control sheep. Cortical mitochondrial function was altered in septic sheep with a reduced respiratory control ratio (6.0 ± 1.5 vs. 8.2 ± 1.6, P = 0.006) and increased complex II-to-complex I ratio during state 3 (1.6 ± 0.2 vs. 1.3 ± 0.1, P = 0.0014) mainly due to decreased complex I-dependent state 3 respiration (P = 0.016). However, no differences in renal mitochondrial efficiency or mitochondrial uncoupling were found. In conclusion, renal mitochondrial dysfunction composed of a reduction of the respiratory control ratio and an increased complex II/complex I relation in state 3 was demonstrated in an ovine model of SA-AKI. However, the disturbed relation between renal $\dot{V}O_2$ and renal Na^+ transport could not be explained by a change in renal cortical mitochondrial efficiency or uncoupling.

NEW & NOTEWORTHY We studied the function of renal cortical mitochondria in relation to oxygen consumption in an ovine model of sepsis with acute kidney injury. We demonstrated changes in the electron transport chain induced by sepsis consisting of a reduced respiratory control ratio mainly by a reduced complex I-mediated respiration. Neither an increase in mitochondrial uncoupling nor a reduction in mitochondrial efficiency was demonstrated and cannot explain why oxygen consumption was unaffected despite reduced tubular transport.

acute kidney injury; mitochondria; sepsis

INTRODUCTION

Sepsis-associated acute kidney injury (SA-AKI) commonly complicates sepsis and septic shock. Targeted interventions to prevent or decrease occurrence and severity are still largely lacking (1). Renal mitochondrial dysfunction has been proposed as a contributing mechanism in the development of SA-AKI and has been demonstrated in a hypodynamic rodent model where renal blood flow is substantially reduced (2). In large animal models, less is known. One study in a porcine model with prolonged endotoxemia failed to demonstrate any in vitro changes in renal mitochondrial function; another suggested increased proton leak in a model of peritoneal sepsis without impaired renal function (3, 4).

Sheep are susceptible to developing renal impairment during experimental sepsis despite normal to increased renal oxygen delivery, in contrast to the previously accepted

Correspondence: T. Luther (tomas.luther@surgsci.uu.se).
Submitted 1 December 2022 / Revised 31 March 2023 / Accepted 19 April 2023

 1931-857X/23 Copyright © 2023 the American Physiological Society.

Downloaded from journals.physiology.org/journal/ajprenal at Uppsala Universitetsbibliotek (130.238.188.192) on September 1, 2023.

hypothesis, in which hypoperfusion was considered an essential contributor to septic SA-AKI (5, 6). This is consistent with a common clinical scenario, in which AKI develops despite the absence of shock (7). Resuscitated septic sheep often develop hyperdynamic circulation, similar to patients in the intensive care unit, and are frequently used to study SA-AKI during these conditions. In ovine models, changes in renal lactate/pyruvate have been demonstrated, although intracellular levels of ATP are preserved, indicating a possibility of mitochondrial dysfunction (5, 8). The effects on cellular homeostasis and function are, however, unclear. A role of altered renal mitochondrial function in sepsis by reducing cellular metabolic demands has been suggested (9). This clearly contrasts observations in septic patients where renal oxygen consumption ($\dot{V}O_2$) is maintained (10). Preserved renal $\dot{V}O_2$ has also been demonstrated in ovine models (11, 12). Also, in patients with AKI in the intensive care unit, a disturbed relation between renal $\dot{V}O_2$ and renal Na^+ transport, which is a major source of ATP demand, has been demonstrated (13, 14). An increase in mitochondrial uncoupling and reduced efficiency could explain a disturbed relationship between $\dot{V}O_2$ and ATP-demanding Na^+ transport, but this has not been investigated.

In this study, we aimed to investigate the function of isolated renal mitochondria compared with renal oxygen handling in an ovine model of hyperdynamic SA-AKI.

METHODS

This study was conducted at dedicated animal research facilities at Uppsala University and the Swedish University of Agricultural Sciences in Uppsala, Sweden. Approval for the study was obtained in advance from the Regional Ethics Committee for Experiments in Animals, Uppsala, Sweden (C60/16 with Amendments 5.8.18-02074/2017 and 5.8.18-14384/2017), and all animals were handled in accordance with directives from the European Commission for Animal Research. This study adhered to the minimum quality threshold in preclinical sepsis studies (MQTIPSS) and Animal Research: Reporting of In Vivo Experiments 2.0 (15, 16).

Anesthesia and Surgical Preparation

Adult *Ovis aries* mixed breed ewes were cannulated in the external jugular vein and anesthetized with 1 g of sodium pentothal intravenously. Following tracheal intubation, normoventilation was established (Flow-i Anesthesia system, Maquet Getinge Group, Solna, Sweden). Positive end-expiratory pressure was set to 5 cmH_2O, tidal volume was set to 8 $mL{\cdot}kg^{-1}$, and the fraction of inspired oxygen was set to 40%. A bolus of 10 mg of morphine was administered intravenously, and anesthesia was maintained with sevoflurane at 2–2.5% end-tidal concentration. A continuous infusion of midazolam (0.1 $mg{\cdot}kg^{-1}{\cdot}h^{-1}$) and morphine (0.26 $mg{\cdot}kg^{-1}{\cdot}h^{-1}$) mixed in 10% buffered glucose was administered at a rate of 2 $mL{\cdot}kg^{-1}{\cdot}h^{-1}$ throughout the experiment. An arterial catheter, a central venous catheter, and a pulmonary artery catheter were inserted for circulatory monitoring and blood sampling in the left carotid artery and via the right jugular vein, respectively. Surgical preparation was then followed by a subcapsular renal biopsy using a 5-mm skin punch (Integra Life, Billerica, MA) placed in an ice-cold mitochondrial isolation medium (17). An ultrasound flow probe (PS-series 4 mm, Transonic Systems, Ithaca, NY) was placed around the left renal artery for renal hemodynamic monitoring, and a renal vein catheter (4-Fr Careflow Arterial Catheter, Merit Medical Systems, South Jordan, UT) was placed using the Seldinger technique at the visualized renal hilum to enable measurements of arterial-venous differences across the kidney. A urinary catheter was inserted for urine sampling and urine output measurements. Once the surgical preparation was finished, a 1-h recovery period ensued before the experimental protocol was initiated. Animals were placed in a prone position at the start of the recovery period and throughout the experiment. Further anesthesia was continued using an infusion of midazolam, morphine, and either inhaled sevoflurane or a continuous infusion of Propofol (20 $mg{\cdot}mL^{-1}$, Braun, Melsungen, Germany) titrated to nonresponsiveness of painful stimuli. Extra doses of analgesics (morphine and ketamine) were administered if signs of unsatisfactory analgesia occurred.

Bacterial Preparation

A live *Escherichia coli* clinical isolate strain (B09-11822) was prepared as a bacterial solution. Bacteria were harvested 1 day in advance and after 60 min of activation in Luria broth and resuspended in saline, resulting in an *E. coli* bacterial solution at a concentration of $\sim 3.4 \times 10^8$ colony-forming $units{\cdot}mL^{-1}$.

Experimental Protocol

The sheep were allocated to one of two groups (sepsis or control groups) after a pilot period by pairwise block randomization with selection by lot balanced to compensate for exclusions and terminations before the planned end of the protocol. Controls served as a means of excluding major effects from the anesthesia and instrumentation alone. Ewes in the sepsis group were administered an intravenous *E. coli* infusion starting at 0.005 $mL{\cdot}kg^{-1}{\cdot}h^{-1}$ after the initial 1-h recovery period. The infusion was increased at 6- to 12-h increments depending on the physiological response. The intervention was not blinded to the investigators.

Fluid therapy was initiated at induction with a 30 $mL{\cdot}kg^{-1}$ bolus of Ringers-acetate (Baxter Medical, Deerfield, IL) and then continued at a maintenance rate of 2 $mL{\cdot}kg^{-1}{\cdot}h^{-1}$ throughout the experiment. Perioperative blood loss was also replaced by Ringers-acetate at a 1:1 ratio. To resemble a human intensive care setting, animals were provided fluid boluses at a predetermined fall in cardiac output, hypotension measured as mean arterial pressure < 60 mmHg was treated with norepinephrine, and positive end-expiratory pressure and fraction of inspired oxygen were increased stepwise when arterial P_{O_2} fell below 10 kPa and minute ventilation was adjusted to maintain P_{CO_2} between 4.5 and 6.5 kPa.

Hemodynamic and respiratory parameters were collected at baseline and at 6-h intervals throughout the experiment. Urine output was registered every 2 h, and urine samples collected every 6 h drawn from the urine were collected during the

Downloaded from journals.physiology.org/journal/ajprenal at Uppsala Universitetsbibliotek (130.238.188.192) on September 1, 2023.

previous 2 h. Blood samples were extracted from the arterial catheter (~20 mL) at the commencement of the experiment and then every 6 h and analyzed at the clinical laboratory at Uppsala University Hospital. Arterial, pulmonary arterial, and renal vein samples were collected at least every 6 h and analyzed with blood gas analyzers at the research facilities (ABL 700 and 835, Radiometer, Copenhagen, Denmark).

After 29 h, a late subcapsular biopsy was taken and the ewes were euthanized by an intravenous dose of potassium chloride. The left kidney was harvested directly postmortem. Renal cortical tissue samples were fixated in 4% formalin and 2% glutaraldehyde in PBS. If ewes deteriorated premorbidly in cardiopulmonary function before the end of the protocol, with pulmonary hypertension (mean pulmonary arterial pressure > 35 mmHg) and decreasing cardiac output despite increasing resuscitative measures, a mitochondrial biopsy was taken, and the ewes were then euthanized before the planned end of the protocol.

Calculations

Arterial and venous oxygen content (Ca_{O_2} and Cv_{O_2}) were calculated using the fraction of oxyhemoglobin (which disregards deoxyhemoglobin, methemoglobin, and hemoglobin bound to carbon monoxide) using the following formula:

$$\text{Oxygen content}\ (\text{mL O}_2\cdot\text{mL}^{-1}) = \left(\left[\text{hemoglobin}\ (\text{g}\cdot\text{dL}^{-1})\right]\times\text{saturation}\times 1.34 + \text{arterial}\ \text{Po}_2(\text{kPa})\times 0.023\right)\times 0.01$$

Renal oxygen delivery and $\dot{V}o_2$ were determined using the following formulas:

$$\text{Left renal oxygen delivery} = Ca_{O_2}\times\ \text{renal blood flow}$$

$$\text{Left renal}\ \dot{V}o_2 = (Ca_{O_2} - Cv_{O_2})\times\text{renal blood flow}$$

Left renal vascular resistance was calculated using mean arterial pressure − central venous pressure as ΔP.

Renal creatinine clearance and Na^+ transport were calculated using the following formulas; left renal Na^+ transport was approximated using total Na^+ transport divided by 2:

$$\text{Creatinine clearance} = \text{urine output}\ (\text{mL}\cdot\text{min}^{-1}) \times \text{U-creatinine}\ (\text{mmol}\cdot\text{L}^{-1}) / (\text{P-creatinine}\ (\text{mol}\cdot\text{L}^{-1}) \times 1{,}000$$

$$\text{Na}^+\text{transport}\ (\text{mmol}\cdot\text{min}^{-1}) = \text{P-Na}\ (\text{mmol}\cdot\text{L}^{-1}) \times \text{creatinine clearance}\ (\text{mL}\cdot\text{min}^{-1}) \times 0.001 - \text{U-Na}\ (\text{mmol}\cdot\text{L}^{-1}) \times \text{urine output}\ (\text{mL}\cdot\text{min}^{-1}) \times 0.001$$

Mitochondrial Function

Biopsies from the kidney cortex were extracted, and mitochondria were isolated by differential centrifugation, as previously described (17). Mitochondrial function was evaluated by high-resolution respirometry at 37°C (Oroboros 2-K, Innsbruck, Austria) in respiration medium containing EGTA (0.5 mM), $MgCl_2 \cdot 6\ H_2O$ (3 mM), K-lactobionate (60 mM), taurine (20 mM), KH_2PO_4 (10 mM), HEPES (20 mM), sucrose (110 mM), and BSA (essentially fatty acid free, 1 $g \cdot L^{-1}$, pH 7.1). Respiration was normalized to mitochondrial protein assessed by a commercial kit (DC Protein Assay, Bio-Rad). The respiratory control ratio (RCR) was defined as maximal complex I-mediated oxidative phosphorylation capacity (state 3) [pyruvate (5 mM), malate (2 mM), and ADP (2.5 mM)] divided by leak state (state 2) without adenylates present (pyruvate and malate). Maximal oxidative phosphorylation capacity was measured in the presence of pyruvate, malate, and succinate (5 mM) followed by the addition of rotenone (0.5 μM) for complex II-dependent state 3. The relation between complex I and complex II was calculated as complex II-dependent state 3 divided by complex I-mediated state 3. The succinate control ratio was calculated as state 3 with succinate (complex I + complex II) divided by complex I-mediated State 3. Leak respiration was measured in the presence of pyruvate, malate, and oligomycin (25 μM). Uncoupling protein 2- and adenine nucleotide translocase-dependent proton leak was estimated by adding GDP (2 mM) and carboxyatractyloside (CAT) (5 μM), respectively. The GDP effect and CAT effect were calculated as leak − GDP and leak − CAT. The P-to-O ratio was measured (in the presence of complex I substrates and 2 mM ATP) by steady-state infusion (14 $nL \cdot s^{-1}$) of a known concentration of ADP, which better mimics the in vivo situation compared with the ADP bolus dose method. The number of mitochondria was set so that the respiration during the ADP infusion corresponded to approximately half-maximal state 3 respiration. Background correction was performed to control for infused oxygen present in the solution. The concentration of ADP in the infusion solution was determined spectrophotometrically with a commercially available kit (MAK081, Merck).

Transmission Electron Microscopy

Small pieces from the kidney cortex were cut and placed in 2% glutaraldehyde and 2% paraformaldehyde in 0.1 M phosphate buffer (pH 7.4) at room temperature and stored at 4°C. Specimens were rinsed in 0.1 M phosphate buffer (pH 7.4) and postfixed in 2% osmium tetroxide and 0.1 M phosphate buffer (pH 7.4) at 4°C for 2 h and dehydrated in ethanol followed by acetone and embedded in LX-112 (Ladd, Burlington, VT). Ultrathin sections (~60–80 nm) were cut by a Leica EM UC 6 (Leica, Wien, Austria) and contrasted with uranyl acetate followed by lead citrate and examined in a Hitachi HT 7700 (Tokyo, Japan) at 80 kV. Digital images were taken using a Veleta camera (Olympus Soft Imaging Solutions, Munster, Germany) (18). Three randomly selected glomeruli were examined in each specimen, and the mitochondria morphology in podocytes was imaged at a final magnification of ×15,000. Mitochondrial morphology was similarly examined in a random sample of three animals in the sepsis group and three in the control group, in which five randomly selected tubuli were examined. Podocytes were chosen for a more thorough evaluation due to their stability after fixation by immersion and density in mitochondria.

Downloaded from journals.physiology.org/journal/ajprenal at Uppsala Universitetsbibliotek (130.238.188.192) on September 1, 2023.

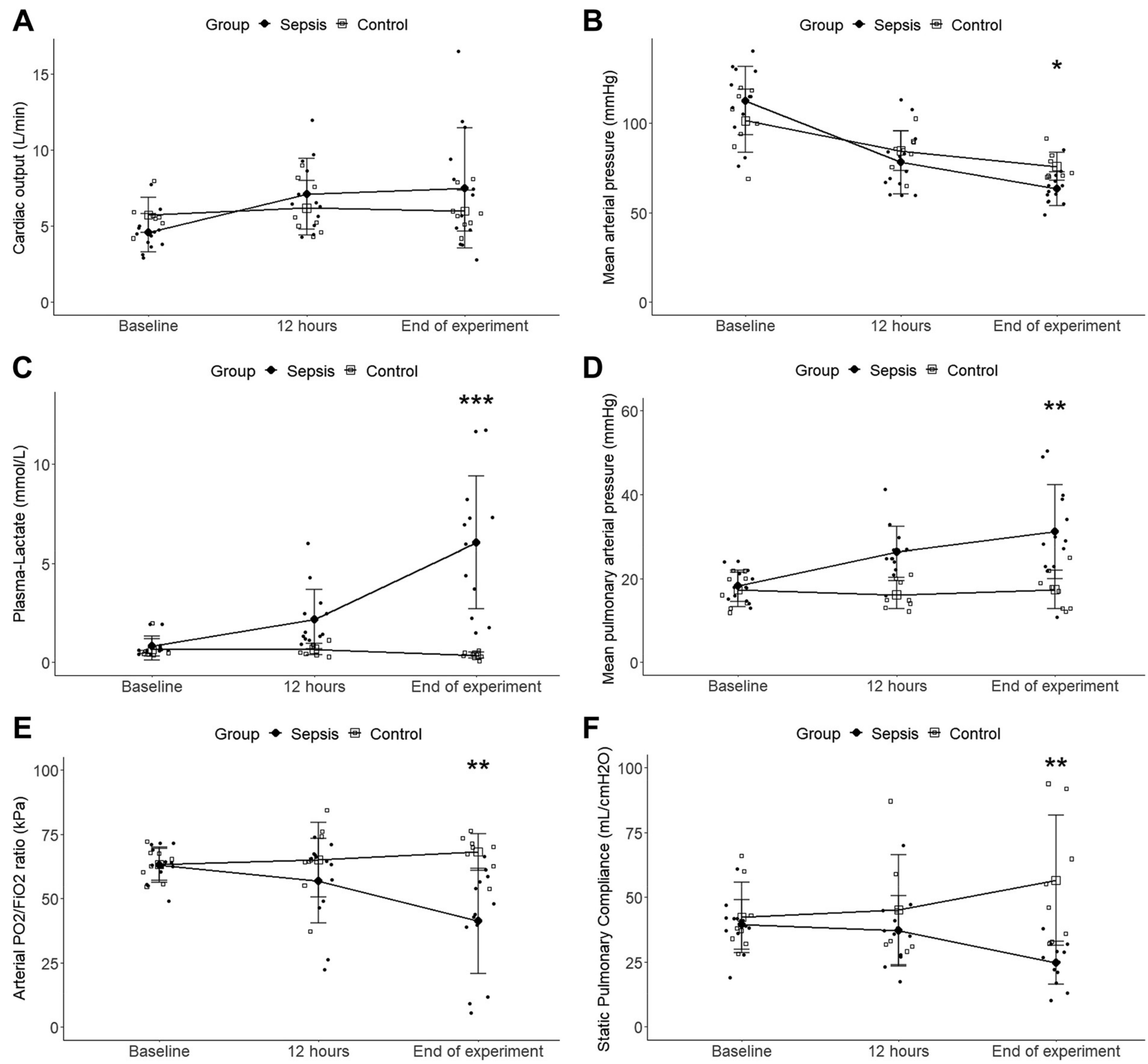

Figure 1. Physiological variables expressed groupwise at three different times during the experiment (at baseline, at 12 h, and at the end of the experiment). *A–F*: cardiac output (*A*), mean arterial pressure (*B*), plasma lactate (*C*), mean pulmonary arterial pressure (*D*), arterial P_{O_2}-to-fraction of inspired oxygen ($F_{I_{O_2}}$) ratio (*E*), and static pulmonary compliance (*F*). n = 13 animals in the sepsis group and n = 8 animals in the control group except in *A* and *F*, where n = 7 animals in the control group. Lines indicate group means and error bars indicate SDs. Observations are marked as symbols from 13 animals in the sepsis group and 8 animals in the control group in *B–E* and from 13 animals in the sepsis group and 7 animals in the control group in *A* and *F*. $^*P < 0.05$, $^{**}P < 0.01$, and $^{***}P < 0.001$ for an interaction effect with repeated-measures ANOVA.

Statistical Analysis

Continuous variables are expressed as means and SD if not stated otherwise. Formal analysis was made using repeated-measures two-way ANOVA with group allocation as between effects and time as within effects. The times chosen for mitochondrial assay were baseline and the end of the experiment. For physiological measurements, baseline, 12 h, and the end of the experiment were used. The last recorded value was used in prematurely euthanized ewes. Where a significant interaction effect was present, planned comparisons at baseline and the end of the experiment were made. Statistica 13 (StatSoft, Hamburg, Germany) 64-bit software was used for calculations. *P* values of <0.05 were considered significant. Missing values before the end of the experiment required for hypothesis testing were imputated as group means at baseline or derived from related intraindividual measurements when possible and accounted for in RESULTS. Missing values of descriptive variables were excluded. Graphs were made using SigmaPlot 14.0 and the ggplot2 package in R 4.1.2.

RESULTS

A total of 21 animals were included in the final analysis, after exclusion of four sheep due to deterioration after instrumentation (2 sheep) or damaged mitochondrial samples during handling (1 control and 1 sepsis). The full predefined course of the experiment was completed by eight animals in the control group and eight animals in the sepsis group. Of the 13 sheep in the sepsis group, five sheep were terminated

Downloaded from journals.physiology.org/journal/ajprenal at Uppsala Universitetsbibliotek (130.238.188.192) on September 1, 2023.

prematurely after mean of 22 ± 2.5 h due to irreversible cardiopulmonary deterioration. Eight animals in the control group and eight animals in the sepsis group completed the full predefined course of the experiment. The anesthesia regiment was comparable between groups (propofol + sevoflurane, n = 4 + 4 in the control group and n = 6 + 7 in the sepsis group).

Effects on Systemic Circulation and Respiration

All septic animals developed signs of septic shock with hemodynamic effects (Fig. 1, *A*–D and Table 1). At the end of the experiment, the sepsis group compared with the control group had similar cardiac output [7.5 ± 4.0 vs. 6.0 ± 1.3 L·min^{-1}, not significant (NS)], a reduction in mean arterial pressure (63 ± 9 vs. 76 ± 8 mmHg, P = 0.006), similarly preserved mixed venous saturation (73 ± 18 vs. 74 ± 4, NS), and increased serum lactate (6.0 ± 3.3 vs. 0.4 ± 0.2, P = 0.0002). Sixty-nine percent of the ewes in the sepsis group received norepinephrine for hypotension at mean of 9.6 ± 5.4 h at a maximum dose of 0.51 ± 0.82 µg·kg^{-1}·min^{-1} compared with none in the control group. Septic ewes showed deteriorating respiratory status according to a reduced P-to-F ratio and decreased pulmonary compliance (Fig. 1, *E* and *F*).

Table 1. *Additional physiological and renal variables expressed groupwise at three different times during the experiment*

	Baseline	12 h	End of Experiment	ANOVA (Interaction Effect)	n
Weight, kg					
Sepsis	56 ± 12				13
Control	50 ± 17				8
Cumulative volume of fluid boluses, mL					
Sepsis			690 ± 1,317		13
Control			254 ± 310		8
Arterial saturation, %					
Sepsis	97 ± 1	97 ± 1	91 ± 12	NS	13
Control	96 ± 1	96 ± 1	96 ± 1		8
Peak inspiratory pressure, cmH_2O					
Sepsis	20 ± 3	21 ± 4	29 ± 8	‡	12
Control	19 ± 4	18 ± 3	18 ± 4		8
Minute ventilation, L·min^{-1}					
Sepsis	8.2 ± 2	7 ± 1.6	8 ± 2.4	‡	12
Control	8.2 ± 1.3	8.1 ± 1.2	5.2 ± 0.7		7
Heart rate, beats·min^{-1}					
Sepsis	107 ± 15	107 ± 11	127 ± 37	†	13
Control	109 ± 11	90 ± 12	80 ± 11		8
Systemic vascular resistance, dyn·s·cm^{-5}					
Sepsis	2,000 ± 634	856 ± 219	668 ± 217	‡	11
Control	1,371 ± 328	1,126 ± 368	981 ± 209		7
Pulmonary artery wedge pressure, mmHg					
Sepsis	10 ± 3	13 ± 3	12 ± 3	NS	11
Control	9 ± 3	9 ± 2	9 ± 3		7
Central venous pressure, mmHg					
Sepsis	5 ± 2	8 ± 4	11 ± 3	*	11
Control	3 ± 3	4 ± 3	5 ± 3		8
Central venous saturation, %					
Sepsis	70 ± 7	78 ± 5	73 ± 18	NS	12
Control	70 ± 6	69 ± 5	74 ± 4		7
Blood hemoglobin, g·L^{-1}					
Sepsis	76 ± 10	96 ± 15	107 ± 29	‡	13
Control	75 ± 13	77 ± 15	69 ± 15		8
Core temperature, °C					
Sepsis	38.5 ± 0.4	39.2 ± 1.1	40.0 ± 1.3	†	13
Control	38.1 ± 0.5	39.3 ± 0.9	38.7 ± 0.6		8
Urine output, mL·min^{-1}					
Sepsis	1.5 ± 1.4	0.8 ± 0.6	0.2 ± 0.1	NS	12
Control	2.3 ± 2.8	3 ± 2.5	2.2 ± 1.6		8
Left renal oxygen delivery, mL·min^{-1}					
Sepsis	22 ± 11	29 ± 16	33 ± 24	NS	13
Control	25 ± 10	26 ± 12	23 ± 10		8
Left renal vascular resistance, mmHg·min·L^{-1}					
Sepsis	0.61 ± 0.24	0.32 ± 0.12	0.32 ± 0.21	*	11
Control	0.47 ± 0.25	0.37 ± 0.14	0.34 ± 0.14		8
Left renal venous saturation, %					
Sepsis	81 ± 9	81 ± 10	80 ± 19	NS	12
Control	82 ± 8	83 ± 6	86 ± 3		8
Plasma Na^+, mmol·L^{-1}					
Sepsis	138 ± 2	134 ± 4	130 ± 5	NS	13
Control	138 ± 2	133 ± 4	131 ± 6		8

Values are represented as means ± SD; n is the number of animals in the analysis. ANOVA indicates the result of an interaction effect in repeated-measures ANOVA. *$P < 0.05$, †$P < 0.01$, ‡$P < 0.001$. NS, not significant.

Downloaded from journals.physiology.org/journal/ajprenal at Uppsala Universitetsbibliotek (130.238.188.192) on September 1, 2023.

Renal Functional Effects

Creatinine clearance decreased significantly in septic animals during the course of the experiment (84 ± 32 vs. 6 ± 5 mL·min^{-1}, $P < 0.0001$) and compared with controls, where the reduction was limited (79 ± 30 vs. 70 ± 36 mL·min^{-1}, NS). Sepsis was not associated with renal hypoperfusion since mean left renal blood flow was preserved in septic ewes throughout the experiment with mean blood flows similar to control ewes (Fig. 2*B*). Renal $\dot{V}O_2$ was unaffected, with a mean left renal $\dot{V}O_2$ of 3.6 ± 1.6 mL·min^{-1} in the sepsis group and 3.5 ± 1.5 mL·min^{-1} in the control group at the end of the experiment (NS). Renal Na^+ transport was substantially reduced in sheep with sepsis, in which mean Na^+ transport at the end of the experiment was 0.8 ± 0.7 mmol·min^{-1} compared with 9 ± 5 mmol·min^{-1} in the control group ($P <$ 0.001). Septic sheep also developed a decreased relation between Na^+ transport in relation to renal $\dot{V}O_2$, with a markedly lower mean Na^+ transport per milliliter consumed oxygen at the end of the experiment compared with controls (0.1 ± 0.1 vs. 1.4 ± 0.8 mmol·mL^{-1}, $P < 0.0001$). Additional renal parameters are shown in Table 1 and Fig. 2, *A*–*F*.

Renal Mitochondrial Assay

RCR was reduced at the end of the experiment in the sepsis group compared with the control group, indicating a disturbance in renal mitochondrial coupling (6 ± 1.5 vs. 8.2 ± 1.6, P = 0.006; Fig. 3*A*). There was also a reduced complex I-mediated state 3 capacity (Fig. 3*C*) at the end of the experiment compared with baseline in septic animals (1.8 ± 0.4 vs. 1.5 ± 0.6 pmol·s^{-1}·µg^{-1}, P = 0.002), whereas no significant

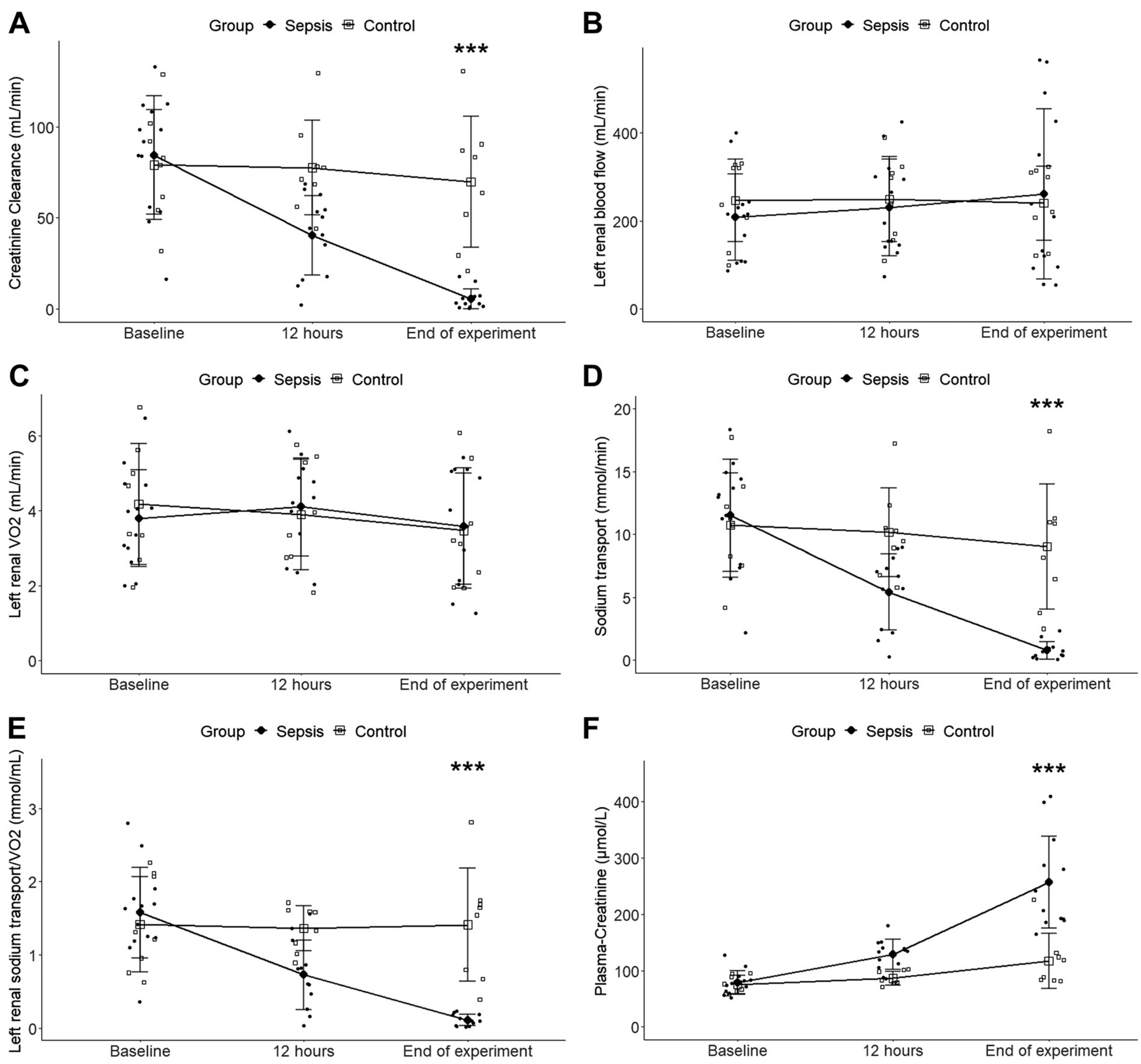

Figure 2. Renal variables expressed groupwise at three different times during the experiment (at baseline, at 12 h, and at the end of the experiment) *A*–*F*: creatinine clearance (*A*), left renal blood flow (*B*), left renal $\dot{V}O_2$ (*C*), sodium transport (*D*), left renal sodium transport/$\dot{V}O_2$ (*E*), and P-creatinine (*F*). Lines indicate group means and error bars indicate SDs. Observations are marked as dots from 13 animals in the sepsis group and 8 animals in the control group in *A*, *B*, and *F* and from 12 animals in the sepsis group and 8 animals in the control group in *C*–*E*. ***$P < 0.001$ for an interaction effect with repeated-measures ANOVA. $\dot{V}O_2$, oxygen consumption.

Downloaded from journals.physiology.org/journal/ajprenal at Uppsala Universitetsbibliotek (130.238.188.192) on September 1, 2023.

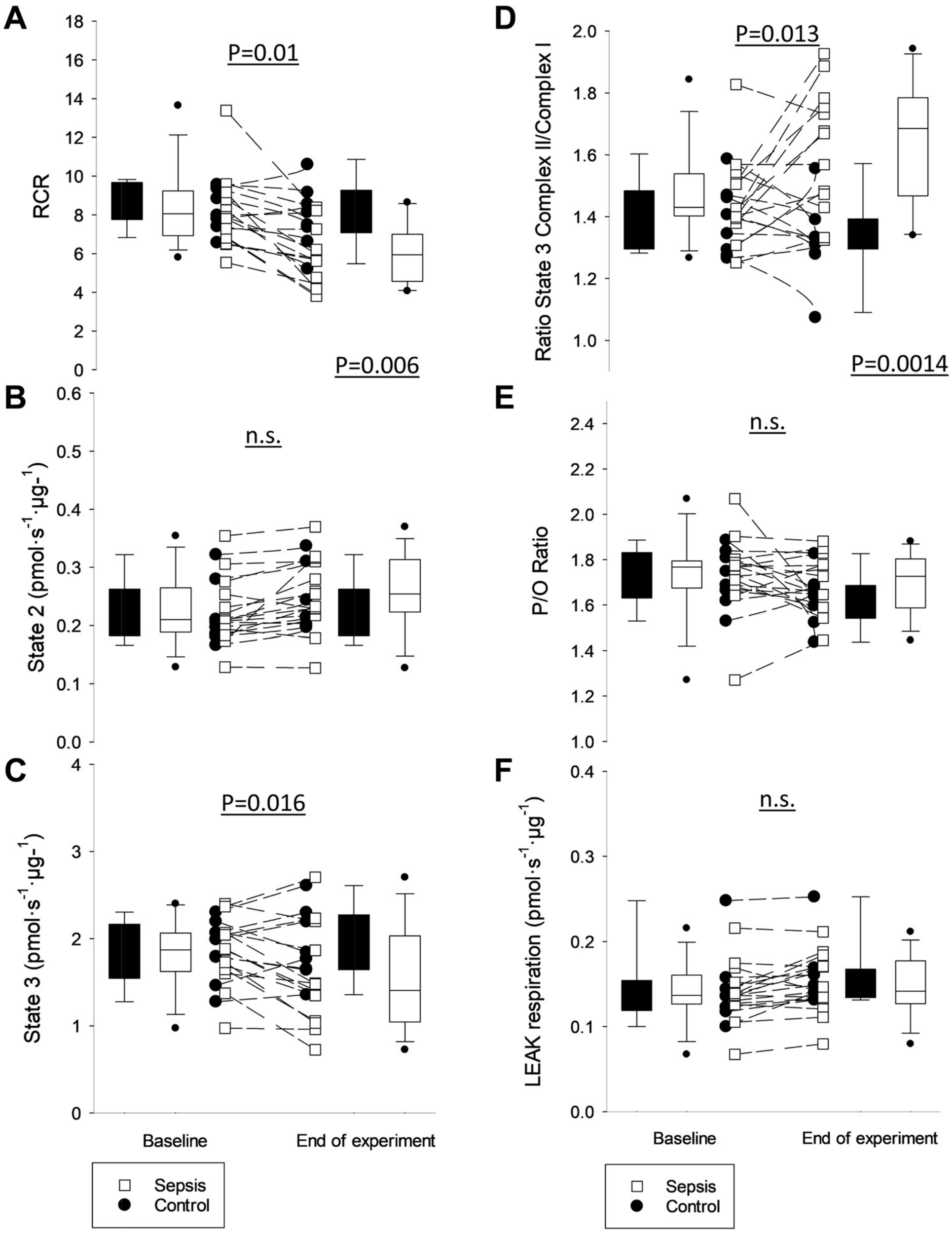

Figure 3. Results of mitochondrial parameters. The respiratory control ratio (RCR) (*A*), state 2 (*B*), state 3 (*C*), complex II/complex I (*D*), P-to-O (P/O) ratio (*E*), and proton leak (*F*) at baseline and the end of the experiment are shown for the sepsis group (n = 13) and control group (n = 8). Results are presented as both boxplots (ends) and individual data points (between), where dashed lines indicate intraindividual changes. The header indicates the results of an interaction effect with ANOVA. P values from post hoc tests between groups are shown below the boxplot for $P < 0.05$. n.s., not significant.

difference in state 2 (Fig. 3*B*) could be demonstrated. The complex II-complex I state 3 ratio increased at the end of the experiment in the sepsis group but not in the control group (1.6 ± 0.2 vs. 1.3 ± 0.1, P = 0.002; Fig. 3*D*), mainly due to the reduction in complex I activity in the sepsis group at the end of the experiment. This was supported by a similar, but not significant, pattern in succinate control ratio (complex I + II/complex I, P = 0.052 by ANOVA; Table 2). No differences in mitochondrial efficiency (P-to-O ratio with complex I substrates) or in mitochondrial uncoupling (leak

Table 2. *Additional mitochondrial assay results*

Variable	ANOVA	Group	Baseline	End of Experiment
Succinate control ratio	NS	Sepsis	1.8 ± 0.1	1.9 ± 0.2
		Control	1.7 ± 0.1	1.7 ± 0.1
GDP-sensitive respiration, pmol·s^{-1}·µg^{-1}	NS	Sepsis	0.007 ± 0.004	0.004 ± 0.003
		Control	0.006 ± 0.003	0.004 ± 0.004
Carboxyatractyloside-sensitive respiration, pmol·s^{-1}·µg^{-1}	NS	Sepsis	0.013 ± 0.008	0.015 ± 0.006
		Control	0.02 ± 0.01	0.023 ± 0.013

Values are presented groupwise for sepsis (13 animals) and control (8 animals) as means ± SD. ANOVA indicates the result of an interaction effect in repeated-measures ANOVA. NS, not significant.

Downloaded from journals.physiology.org/journal/ajprenal at Uppsala Universitetsbibliotek (130.238.188.192) on September 1, 2023.

respiration) could be demonstrated (Fig. 3, *E* and *F*). Additional results are further shown in Table 2.

Mitochondrial Morphology in the Cortex

Mitochondrial morphology was examined in podocytes in three randomly selected glomeruli in all included ewe cortical biopsies. No pathological ultrastructural changes were observed in any of the animals (Fig. 4). Furthermore, mitochondrial morphology was examined in five randomly selected tubuli in three animals from the sepsis group and three animals in the control group. No differences between the groups were found. However, some morphological artifacts in tubular cells, in general, were noted, due to the insufficiency of the fixation by immersion.

Missing Data

In one septic ewe terminated before the planned end, renal vein samples were unavailable after baseline measurement and excluded from the analysis of affected variables. Two correct baseline measurements of creatinine clearance and Na^+ transport were missing (1 in the sepsis group and 1 in the control group) and were imputed as respective group means. In regard to one ewe in the sepsis group that was euthanized early, mitochondrial state 3 respiration with rotenone was missing at baseline and was imputed as the group mean.

DISCUSSION

The main result of the present study is that renal mitochondrial dysfunction composed of a reduction of RCR and a disturbance in the relation between complex I and complex II activity in state 3 can be demonstrated in an ovine model of SA-AKI. Also, the decreased relation between renal $\dot{V}O_2$ and renal Na^+ transport cannot be explained by a change in renal mitochondrial efficiency or by renal mitochondrial uncoupling.

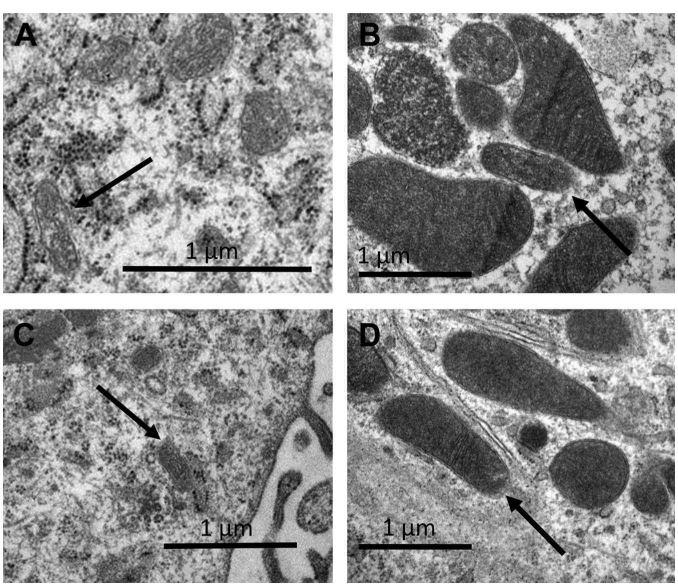

Figure 4. Transmission electron microscopy images of mitochondria in podocytes and tubular cells from ewes at the end of the experiment. *A* and *B*: mitochondria in podocytes from one ewe from the control group (*A*) and from one ewe from the sepsis group (*B*). *C* and *D*: mitochondria in tubuli from one ewe from the control group (*C*) and from one ewe from the sepsis group (*D*). Podocytes from all included animals, as well as tubuli from a random sample of 3 + 3 animals in the control and sepsis groups, respectively, were examined without any morphological differences between groups. Scale bars = 1 µm.

In our study, the reduction of RCR and decreased relation between complex I and complex II was mainly driven by reduced complex I-dependent state 3 respiration induced by infusion of live *E. coli*. This is in contrast to a previous large-animal study in septic pigs where a state 2 reduction was the main finding (4); however, it was not associated with a decrease in creatinine clearance. Reduced complex I activity has been demonstrated in animal models of sepsis (3, 19). In patients in intensive care with septic shock, reduced complex I activity in skeletal muscle was associated with increased norepinephrine requirements and decreased survival (20). This is considered a result of prolonged nitric oxide (NO) exposure, which induces complex I inhibition, both reversibly and irreversibly (21). This effect is also ameliorated by the inhibition of NO synthase (NOS) (22). The renal mitochondrial effects of NO are not limited to complex I inhibition. In addition to modulation of cytochrome *c* oxidase, there are effects of NO that may be beneficial in the context of SA-AKI (23). NO promotes mitochondrial stability and inducible NOS depletion, resulting in an accumulation of dysfunctional mitochondria (24). Also, inducible NOS inhibition in large animal models of sepsis has not proven beneficial to renal function (25). Thus, the role of affected renal complex I respiration in the pathogenesis of SA-AKI is still unclear and requires further exploration.

The decreased relation between renal $\dot{V}O_2$ and Na^+ transport demonstrated here is coherent with previous studies in sheep and patients with SA-AKI and postcardiopulmonary bypass-associated AKI and can be considered a feature of AKI in the clinical context (10, 11, 14). A major feature of AKI in septic sheep is decreased glomerular filtration rate, although renal blood flow remains unchanged or is increased, indicating a reduction in filtration fraction (26). This may be caused by a dilation of the efferent arteriole, but glomerular swelling secondary to activation of the innate immune system may also contribute (5, 27). When the glomerular filtration rate declines during AKI, less Na^+ is filtered and less Na^+ is available for transport by tubular cells. Renal Na^+ transport is a major source of ATP demand, where a reduction of the transport results in a reduction of renal $\dot{V}O_2$ by approximately one-third (13). The marked reduction in Na^+ transport during SA-AKI in the present study would thus be expected to decrease renal $\dot{V}O_2$ if no other oxygen-demanding process increased. Renal $\dot{V}O_2$ was uniform throughout the experiment in our study, as previously described by others, and ATP levels have previously been shown to be maintained in this model (8, 12). Mitochondrial uncoupling has been proposed to counteract increased oxidative stress (28). Also, morphological changes in renal mitochondria that could indicate damage and an increased risk of unspecific proton leak have also been described in postmortem biopsies from patients with SA-AKI (29). Our results indicate that it is not likely that the maintained renal $\dot{V}O_2$ is caused by increased mitochondrial proton leak and a reduced P-to-O ratio. This implies renal mitochondria may use oxygen for ATP production with the same efficiency as in nonseptic animals. No morphological changes in

Downloaded from journals.physiology.org/journal/ajprenal at Uppsala Universitetsbibliotek (130.238.188.192) on September 1, 2023.

renal mitochondria were observed. There are other possible explanations for a maintained renal $\dot{V}O_2$. Cell repair may require an increase in ATP demand and infiltrating immune cells have a high energy demand. It has also been demonstrated that the permeability of tight junctions in the epithelium is increased after an ischemic insult (30). This would, in theory, allow Na^+ reabsorbed in the proximal tubule to leak back into the urine, which reduces the metabolic efficacy of the kidney and disenables the possibility to create a concentration gradient of Na^+ between the tubular lumen and interstitium by transcellular transport of Na^+ (31).

Our study has several limitations. Global renal oxygen consumption in contrast to subcapsularly localized mitochondria was studied; hence, no conclusions regarding different regions' mitochondrial function could be drawn. Still, cortical and adjacent tubular mitochondria account for a relevant proportion of renal mitochondria, and regional disturbance as the major contributor to the observed disturbance in the renal $\dot{V}O_2/Na^+$ transport relation is less likely. Furthermore, in vitro assessment of mitochondrial function may not reflect actual intracellular conditions. The P-to-O ratio has been suggested to be higher in vivo than in isolated mitochondria, and proton leak is expected to decrease in vivo with increasing ATP demand (32, 33). Furthermore, a reduced mitochondrial density would not be visible in the analysis of isolated mitochondria. Morphology was examined in the cortex and cannot exclude morphological alterations in medullary or tubular cells. As the cells in the tubuli are more sensitive to degradation after fixation by immersion, the available data come with limitations that prevent firm conclusions. Several functional aspects of mitochondria that are not reflected in respirometry as mitochondrial biogenesis and mitophagy, which both are known to be affected by organ dysfunction in sepsis, have not been evaluated (34, 35). Animals were anesthetized throughout the experiment, which influences parameters such as renal blood flow and aggravates SA-AKI; however, the drugs used are common in intensive care, and our results demonstrate that the effects are not caused by instrumentation and anesthesia alone (36). RCR at baseline was maintained around 8 in both the control group and sepsis group and was not significantly decreased at the end of the experiment in the control group. This suggests that mitochondrial integrity and function were maintained during the isolation procedure (37). Furthermore, these observations suggest that mitochondria were not affected by the long period of anesthesia.

In conclusion, the results of this study indicate that in an ovine model of SA-AKI, renal mitochondria develop a reduction of RCR and a disturbance in the relation between complex I and complex II activity. Furthermore, the decreased relation between renal $\dot{V}O_2$ and renal Na^+ transport cannot be explained by a change in renal mitochondrial efficiency or by renal mitochondrial uncoupling.

DATA AVAILABILITY

Data are available from the corresponding author upon reasonable request.

ACKNOWLEDGMENTS

The graphical abstract was created with BioRender.com.

GRANTS

This work was funded by Swedish Research Council (Vetenskapsrådet) Grants 2014-02569 and 2014-07606 (to R.F.).

DISCLOSURES

No conflicts of interest, financial or otherwise, are declared by the authors.

AUTHOR CONTRIBUTIONS

T.L., S.B.-A., F.P., T.A.S., and R.F. conceived and designed research; T.L., S.B.-A., P.P., S.F., P.S., T.A.S., and R.F. performed experiments; T.L., K.H., A.W., and R.F. analyzed data; T.L., A.W., K.H., F.P., T.A.S., and R.F. interpreted results of experiments; T.L. prepared figures; T.L. drafted manuscript; T.L., S.B.-A., S.F., P.S., K.H., A.W., T.A.S., and R.F. edited and revised manuscript; T.L., S.B.-A., P.P., S.F., P.S., A.W., K.H., F.P., T.A.S., and R.F. approved final version of manuscript.

REFERENCES

1. **Kellum JA, Chawla LS, Keener C, Singbartl K, Palevsky PM, Pike FL, Yealy DM, Huang DT, Angus DC; ProCESS and ProGReSS-AKI Investigators.** The effects of alternative resuscitation strategies on acute kidney injury in patients with septic shock. *Am J Respir Crit Care Med* 193: 281–287, 2016. doi:10.1164/rccm.201505-0995OC.
2. **Tran M, Tam D, Bardia A, Bhasin M, Rowe GC, Kher A, Zsengeller ZK, Akhavan-Sharif MR, Khankin EV, Saintgeniez M, David S, Burstein D, Karumanchi SA, Stillman IE, Arany Z, Parikh SM.** PGC-1α promotes recovery after acute kidney injury during systemic inflammation in mice. *J Clin Invest* 121: 4003–4014, 2011. doi:10.1172/JCI58662.
3. **Porta F, Takala J, Weikert C, Bracht H, Kolarova A, Lauterburg BH, Borotto E, Jakob SM.** Effects of prolonged endotoxemia on liver, skeletal muscle and kidney mitochondrial function. *Crit Care* 10: R118, 2006. doi:10.1186/cc5013.
4. **Kozlov AV, van Griensven M, Haindl S, Kehrer I, Duvigneau JC, Hartl RT, Ebel T, Jafarmadar M, Calzia E, Gnaiger E, Redl H, Radermacher P, Bahrami S.** Peritoneal inflammation in pigs is associated with early mitochondrial dysfunction in liver and kidney. *Inflammation* 33: 295–305, 2010. doi:10.1007/s10753-010-9185-4.
5. **Fenhammar J, Rundgren M, Hultenby K, Forestier J, Taavo M, Kenne E, Weitzberg E, Eriksson S, Ozenci V, Wernerson A, Frithiof R.** Renal effects of treatment with a TLR4 inhibitor in conscious septic sheep. *Crit Care* 18: 488, 2014. doi:10.1186/s13054-014-0488-y.
6. **Schrier RW, Wang W.** Acute renal failure and sepsis. *N Engl J Med* 351: 159–169, 2004. doi:10.1056/NEJMra032401.
7. **Murugan R, Karajala-Subramanyam V, Lee M, Yende S, Kong L, Carter M, Angus DC, Kellum JA; Genetic and Inflammatory Markers of Sepsis (GenIMS) Investigators.** Acute kidney injury in non-severe pneumonia is associated with an increased immune response and lower survival. *Kidney Int* 77: 527–535, 2010. doi:10.1038/ki.2009.502.
8. **May CN, Ishikawa K, Wan L, Williams J, Wellard RM, Pell GS, Jackson GD, Bellomo R.** Renal bioenergetics during early gram-negative mammalian sepsis and angiotensin II infusion. *Intensive Care Med* 38: 886–893, 2012. doi:10.1007/s00134-012-2487-2.
9. **Singer M.** The role of mitochondrial dysfunction in sepsis-induced multi-organ failure. *Virulence* 5: 66–72, 2014. doi:10.4161/viru.26907.
10. **Skytte Larsson J, Krumbholz V, Enskog A, Bragadottir G, Redfors B, Ricksten SE.** Renal blood flow, glomerular filtration rate, and renal oxygenation in early clinical septic shock. *Crit Care Med* 46: e560–e566, 2018. doi:10.1097/CCM.0000000000003088.
11. **Weber A, Schwieger IM, Poinsot O, Klohn M, Gaumann DM, Morel DR.** Sequential changes in renal oxygen consumption and sodium transport during hyperdynamic sepsis in sheep. *Am J Physiol Renal Physiol* 262: F965–F971, 1992. doi:10.1152/ajprenal.1992.262.6.F965.
12. **Lankadeva YR, Kosaka J, Evans RG, Bailey SR, Bellomo R, May CN.** Intrarenal and urinary oxygenation during norepinephrine

Downloaded from journals.physiology.org/journal/ajprenal at Uppsala Universitetsbibliotek (130.238.188.192) on September 1, 2023.

resuscitation in ovine septic acute kidney injury. *Kidney Int* 90: 100–108, 2016. doi:10.1016/j.kint.2016.02.017.

13. **Kjekshus J**, **Aukland K**, **Kiil F.** Oxygen cost of sodium reabsorption in proximal and distal parts of the nephron. *Scand J Clin Lab Invest* 23: 307–316, 1969. doi:10.3109/00365516909081696.
14. **Redfors B**, **Bragadottir G**, **Sellgren J**, **Swärd K**, **Ricksten SE.** Acute renal failure is NOT an "acute renal success"—a clinical study on the renal oxygen supply/demand relationship in acute kidney injury. *Crit Care Med* 38: 1695–1701, 2010. doi:10.1097/CCM.0b013e3181e61911.
15. **Osuchowski MF**, **Ayala A**, **Bahrami S**, **Bauer M**, **Boros M**, **Cavaillon JM**, **Chaudry IH**, **Coopersmith CM**, **Deutschman C**, **Drechsler S**, **Efron P**, **Frostell C**, **Fritsch G**, **Gozdzik W**, **Hellman J**, **Huber-Lang M**, **Inoue S**, **Knapp S**, **Kozlov AV**, **Libert C**, **Marshall JC**, **Moldawer LL**, **Radermacher P**, **Redl H**, **Remick DG**, **Singer M**, **Thiemermann C**, **Wang P**, **Wiersinga WJ**, **Xiao X**, **Zingarelli B.** Minimum quality threshold in pre-clinical sepsis studies (MQTiPSS): an international expert consensus initiative for improvement of animal modeling in sepsis. *Infection* 46: 687–691, 2018 [Erratum in *Infection* 46: 745, 2018]. doi:10.1007/s15010-018-1183-8.
16. **Percie Du Sert N**, **Hurst V**, **Ahluwalia A**, **Alam S**, **Avey MT**, **Baker M**, **Browne WJ**, **Clark A**, **Cuthill IC**, **Dirnagl U**, **Emerson M**, **Garner P**, **Holgate ST**, **Howells DW**, **Karp NA**, **Lazic SE**, **Lidster K**, **MacCallum CJ**, **Macleod M**, **Pearl EJ**, **Petersen OH**, **Rawle F**, **Reynolds P**, **Rooney K**, **Sena ES**, **Silberberg SD**, **Steckler T**, **Würbel H.** The ARRIVE guidelines 2.0: updated guidelines for reporting animal research. *PLoS Biol* 18: e3000410, 2020. doi:10.1371/journal.pbio.3000410.
17. **Schiffer TA**, **Gustafsson H**, **Palm F.** Kidney outer medulla mitochondria are more efficient compared with cortex mitochondria as a strategy to sustain ATP production in a suboptimal environment. *Am J Physiol Renal Physiol* 315: F677–F681, 2018. doi:10.1152/ajprenal.00207.2018.
18. **Ruzzenente B**, **Metodiev MD**, **Wredenberg A**, **Bratic A**, **Park CB**, **Cámara Y**, **Milenkovic D**, **Zickermann V**, **Wibom R**, **Hultenby K**, **Erdjument-Bromage H**, **Tempst P**, **Brandt U**, **Stewart JB**, **Gustafsson CM**, **Larsson NG.** LRPPRC is necessary for polyadenylation and coordination of translation of mitochondrial mRNAs. *EMBO J* 31: 443–456, 2012. doi:10.1038/emboj.2011.392.
19. **Brealey D**, **Karyampudi S**, **Jacques TS**, **Novelli M**, **Stidwill R**, **Taylor V**, **Smolenski RT**, **Singer M.** Mitochondrial dysfunction in a long-term rodent model of sepsis and organ failure. *Am J Physiol Regul Integr Comp Physiol* 286: R491–R497, 2004. doi:10.1152/ajpregu.00432.2003.
20. **Brealey D**, **Brand M**, **Hargreaves I**, **Heales S**, **Land J**, **Smolenski R**, **Davies NA**, **Cooper CE**, **Singer M.** Association between mitochondrial dysfunction and severity and outcome of septic shock. *Lancet* 360: 219–223, 2002. doi:10.1016/S0140-6736(02)09459-X.
21. **Clementi E**, **Brown GC**, **Feelisch M**, **Moncada S.** Persistent inhibition of cell respiration by nitric oxide: crucial role of *S*-nitrosylation of mitochondrial complex I and protective action of glutathione. *Proc Natl Acad Sci USA* 95: 7631–7636, 1998. doi:10.1073/pnas.95.13.7631.
22. **Boulos M**, **Astiz ME**, **Barua RS**, **Osman M.** Impaired mitochondrial function induced by serum from septic shock patients is attenuated by inhibition of nitric oxide synthase and poly(ADP-ribose) synthase. *Crit Care Med* 31: 353–358, 2003. doi:10.1097/01.CCM.0000050074.82486.B2.
23. **Cleeter MW**, **Cooper JM**, **Darley-Usmar VM**, **Moncada S**, **Schapira AH.** Reversible inhibition of cytochrome c oxidase, the terminal enzyme of the mitochondrial respiratory chain, by nitric oxide. Implications for neurodegenerative diseases. *FEBS Lett* 345: 50–54, 1994. doi:10.1016/0014-5793(94)00424-2.
24. **Mao K**, **Chen S**, **Chen M**, **Ma Y**, **Wang Y**, **Huang B**, **He Z**, **Zeng Y**, **Hu Y**, **Sun S**, **Li J**, **Wu X**, **Wang X**, **Strober W**, **Chen C**, **Meng G**, **Sun B.** Nitric oxide suppresses NLRP3 inflammasome activation and protects against LPS-induced septic shock. *Cell Res* 23: 201–212, 2013. doi:10.1038/cr.2013.6.
25. **Cohen RI**, **Hassell AM**, **Marzouk K**, **Marini C**, **Liu SF**, **Scharf SM.** Renal effects of nitric oxide in endotoxemia. *Am J Respir Crit Care Med* 164: 1890–1895, 2001. doi:10.1164/ajrccm.164.10.2103140.
26. **Langenberg C**, **Wan L**, **Egi M**, **May CN**, **Bellomo R.** Renal blood flow in experimental septic acute renal failure. *Kidney Int* 69: 1996–2002, 2006. doi:10.1038/sj.ki.5000440.
27. **May CN**, **Calzavacca P**, **Ishikawa K**, **Langenberg C**, **Wan L**, **Ramchandra R**, **Bellomo R.** Novel targets for sepsis-induced kidney injury: the glomerular arterioles and the sympathetic nervous system. *Exp Physiol* 97: 1168–1177, 2012. doi:10.1113/expphysiol.2011.061804.
28. **Sun J**, **Zhang J**, **Tian J**, **Virzì GM**, **Digvijay K**, **Cueto L**, **Yin Y**, **Rosner MH**, **Ronco C.** Mitochondria in sepsis-induced AKI. *J Am Soc Nephrol* 30: 1151–1161, 2019. doi:10.1681/ASN.2018111126.
29. **Takasu O**, **Gaut JP**, **Watanabe E**, **To K**, **Fagley RE**, **Sato B**, **Jarman S**, **Efimov IR**, **Janks DL**, **Srivastava A**, **Bhayani SB**, **Drewry A**, **Swanson PE**, **Hotchkiss RS.** Mechanisms of cardiac and renal dysfunction in patients dying of sepsis. *Am J Respir Crit Care Med* 187: 509–517, 2013. doi:10.1164/rccm.201211-1983OC.
30. **Molitoris BA**, **Falk SA**, **Dahl RH.** Ischemia-induced loss of epithelial polarity. Role of the tight junction. *J Clin Invest* 84: 1334–1339, 1989. doi:10.1172/JCI114302.
31. **Hansell P**, **Welch WJ**, **Blantz RC**, **Palm F.** Determinants of kidney oxygen consumption and their relationship to tissue oxygen tension in diabetes and hypertension. *Clin Exp Pharmacol Physiol* 40: 123–137, 2013. doi:10.1111/1440-1681.12034.
32. **Korzeniewski B.** Contribution of proton leak to oxygen consumption in skeletal muscle during intense exercise is very low despite large contribution at rest. *PLoS One* 12: e0185991, 2017. doi:10.1371/journal.pone.0185991.
33. **Marcinek DJ**, **Schenkman KA**, **Ciesielski WA**, **Conley KE.** Mitochondrial coupling in vivo in mouse skeletal muscle. *Am J Physiol Cell Physiol* 286: C457–C463, 2004. doi:10.1152/ajpcell.00237.2003.
34. **Haden DW**, **Suliman HB**, **Carraway MS**, **Welty-Wolf KE**, **Ali AS**, **Shitara H**, **Yonekawa H**, **Piantadosi CA.** Mitochondrial biogenesis restores oxidative metabolism during *Staphylococcus aureus* sepsis. *Am J Respir Crit Care Med* 176: 768–777, 2007. doi:10.1164/rccm.200701-161OC.
35. **Carré JE**, **Orban JC**, **Re L**, **Felsmann K**, **Iffert W**, **Bauer M**, **Suliman HB**, **Piantadosi CA**, **Mayhew TM**, **Breen P**, **Stotz M**, **Singer M.** Survival in critical illness is associated with early activation of mitochondrial biogenesis. *Am J Respir Crit Care Med* 182: 745–751, 2010. doi:10.1164/rccm.201003-0326OC.
36. **Frithiof R**, **Soehnlein O**, **Eriksson S**, **Fenhammar J**, **Hjelmqvist H**, **Lindbom L**, **Rundgren M.** The effects of isoflurane anesthesia and mechanical ventilation on renal function during endotoxemia. *Acta Anaesthesiol Scand* 55: 401–410, 2011. doi:10.1111/j.1399-6576.2011.02406.x.
37. **Lanza IR**, **Nair KS.** Functional assessment of isolated mitochondria in vitro. *Methods Enzymol* 457: 349–372, 2009. doi:10.1016/S0076-6879(09)05020-4.

Downloaded from journals.physiology.org/journal/ajprenal at Uppsala Universitetsbibliotek (130.238.188.192) on September 1, 2023.